Research Square

Preprints are preliminary reports that have not undergone peer review.
They should not be considered conclusive, used to inform clinical practice,
or referenced by the media as validated information.

Biomechanical response of maxillary All-on-4 systems under different lateral occlusal guidance patterns: a three-dimensional finite element study

Yanrong Song
The Affiliated Stomatological Hospital of Guizhou Medical University
Hongjing Liu
The Affiliated Stomatological Hospital of Guizhou Medical University
Siyang Luo
Guiyang Hospital of Stomatlogy
Xiao Zeng
The Affiliated Stomatological Hospital of Guizhou Medical University
Qiang Dong
dongstrongvv@outlook.com
The Affiliated Stomatological Hospital of Guizhou Medical University

Research Article

Keywords: All-on-4 implants, lateral occlusion, finite element analysis, stress distribution, dental prosthetics

Posted Date: September 14th, 2026

DOI: https://doi.org/10.21203/rs.3.rs-10444228/v1

License: This work is licensed under a Creative Commons Attribution 4.0 International License.
Read Full License

Additional Declarations: No competing interests reported.

Abstract

Background

The All-on-4 concept is widely used for the rehabilitation of edentulous patients; however, the optimal design of lateral occlusal guidance for maxillary All-on-4 prostheses remains unclear. Currently, there is a lack of biomechanical evidence regarding different lateral guidance patterns under varying bone quality conditions.

Methods

A three-dimensional finite element model was created using cone-beam computed tomography and intraoral scanning data from a single healthy volunteer with intact natural dentition and bilateral canine-protected occlusion. Four NobelActive implants (4.3 × 13 mm) were placed in the maxilla according to the All-on-4 protocol. Four lateral occlusal schemes were simulated: canine-protected occlusion, two-tooth group function, three-tooth group function, and posterior group function. Displacement-controlled quasi-static loading was applied to replicate physiological mandibular movements under three bone quality types (D2, D3, and D4, based on Misch classification).

Results

Stress was mainly concentrated at the implant cervical regions and the abutment–implant interfaces. Under D2 bone quality, the abutment at position 12 exhibited a maximum stress of 230.09 MPa in canine-protected occlusion, rising to 259.88 MPa in three-tooth group function. Compared with canine-protected occlusion (113.65 MPa), the maximum implant stress at position 15 under three-tooth group function (165.47 MPa) increased by 45.6%; at position 25, the increase was 75.6% (from 115.14 MPa to 202.23 MPa). Framework deformation increased from 0.0333 mm (D2, canine-protected) to 0.0496 mm (D4, posterior group function), representing a 49% increase.

Conclusions

Canine-protected occlusion effectively reduces stress concentration in implants and composite abutments of the maxillary All-on-4 system. Decreased stress at the implant-abutment interface in lower bone density is accompanied by increased framework deformation. These biomechanical findings suggest that canine-protected occlusion may offer mechanical advantages for maxillary All-on-4 rehabilitation, though clinical implementation should consider individual patient factors.

Background

With the acceleration of population aging, the demand for edentulous jaw rehabilitation has increased significantly. Due to maxillary sinus pneumatization, residual alveolar ridge resorption, and poor bone quality, implant rehabilitation of the edentulous maxilla has long been recognized as a major clinical challenge [1–4]. To avoid bone grafting, reduce surgical trauma, and bypass critical anatomical structures such as the maxillary sinus or inferior alveolar nerve, the All-on-4 implant rehabilitation concept has been proposed [5]. The All-on-4 fixed implant prosthesis employs four implants to support a full-arch fixed bridge with 10–12 units. The distal implants are placed at an angle, allowing a reduced number of implants and the use of distal cantilevers to enhance masticatory efficiency. The long-term clinical outcomes of All-on-4 fixed implant prostheses are closely associated with biomechanical factors [6]. In maxillary All-on-4 rehabilitation, the stress distribution in peri-implant bone surrounding the tilted implant nearest to the distal cantilever remains controversial.

Both masticatory cycles and parafunctional activities generate substantial lateral forces during occlusal load transmission [7]. Notably, in the All-on-4 concept, the prosthesis and implants are rigidly connected as a single unit. Because implants lack the periodontal ligament, a critical structure for force dissipation, occlusal loads are transmitted directly to the jawbone. This uneven stress distribution may lead to bone resorption and biological complications, such as peri-implantitis, potentially resulting in implant loosening and eventual failure [8, 9].

At present, there is no consensus regarding key occlusal issues in All-on-4 implant rehabilitation, including the design of lateral movement patterns, highlighting the need for further investigation. With the increasing integration of medicine and engineering mechanics, three-dimensional finite element analysis has become an advanced and effective research tool in the field of dentistry [10]. The construction of accurate three-dimensional models is a fundamental step in finite element biomechanical analysis. CBCT data enable the development of precise anatomical models for medical research. In this study, CBCT scanning data combined with three-dimensional reconstruction software were used to establish a complete three-dimensional maxillary model, providing a reliable basis for finite element analysis. This study analyzes the effects of different occlusal contact patterns on stress distribution in All-on-4 fixed implant prostheses, providing biomechanical evidence for lateral occlusal design and clinical occlusal adjustment.

Materials and methods

Study Design and Ethical Considerations

This computational biomechanical study was conducted following institutional review board approval and adherence to Declaration of Helsinki principles. A single healthy volunteer provided informed consent for digital imaging and mandibular movement recording procedures.

Subject Selection and Digital Acquisition

A single healthy volunteer with intact natural dentition participated in this investigation. Selection criteria included: symmetric facial morphology and dental arch, normal overbite and overjet relationships, absence of temporomandibular joint disorders, absence of pathological tooth wear, and bilateral canine-protected occlusion.

High-resolution cone-beam computed tomography (CBCT) imaging was performed using a 3D Accuitomo system (Morita Manufacturing Corporation, Japan) with 0.125mm voxel resolution. Scanning parameters included 90kV, 5mA, and 17.5-second exposure time, capturing anatomical structures from bilateral condylar heads to mandibular inferior borders. Digital imaging and communications in medicine (DICOM) format data were acquired for subsequent processing.

Complementary intraoral scanning was performed using an Aoralscan 3w system (SHINING 3D Technology, China) to capture precise occlusal surface geometry, compensating for CBCT resolution limitations in fine anatomical detail. Natural tooth occlusion was digitally replicated with interference elimination and surface verification prior to model assembly.

Three-Dimensional Model Construction

DICOM datasets were imported into Mimics Research 21.0 software (Materialise NV, Belgium) for anatomical segmentation and three-dimensional reconstruction. Individual anatomical structures including cortical bone, cancellous bone, maxillary sinuses, and neurovascular bundles were extracted using threshold-based segmentation algorithms combined with manual refinement techniques (Fig. 1).

Point cloud models generated through segmentation were converted to stereolithography (STL) format for compatibility with computer-aided design software. Surface processing was performed in Geomagic Studio 2021 (3D Systems Corporation, USA) using advanced smoothing algorithms and curvature optimization techniques. Final models were exported in standard for the exchange of product model data (STEP) format to maintain geometric precision across software platforms.

Edentulous maxillary models were created through digital tooth extraction and alveolar bone remodeling simulation, incorporating clinically realistic healing patterns observed in edentulous anatomy. Socket filling and ridge remodeling were performed using Boolean operations and surface sculpting techniques to achieve anatomically appropriate edentulous morphology.

Implant and Prosthetic Component Modeling

Four NobelActive implants (Nobel Biocare AB, Sweden) with 4.3mm diameter and 13mm length were digitally positioned according to established All-on-4 protocols using Solidworks 2023 software (Dassault Systèmes, France). Lateral incisor sites (positions 12 and 22) received vertically oriented implants with 17° multi-unit abutments, while second premolar positions (15 and 25) accommodated 30° angled implants with corresponding 30° multi-unit abutments.

A titanium framework was designed spanning from canine to first molar regions with 7mm distal cantilever extensions. Framework dimensions were optimized for adequate strength while maintaining appropriate prosthetic space. Zirconia crowns were modeled to replicate volunteer tooth morphology with crown heights ranging from 7-9mm and anatomically appropriate emergence profiles.

All prosthetic components were assembled in Solidworks maintaining clinical clearances, proper emergence angles, and physiologically appropriate contact relationships. Assembly constraints ensured accurate spatial relationships between components while allowing for subsequent finite element analysis preparation.

Experimental Group Configuration

Twelve experimental groups were established based on cancellous bone quality classification (D2, D3, D4 according to Misch criteria) [11] and lateral occlusal guidance patterns. The specific configurations are detailed in Table 1.

Table 1
Experimental Group Configuration (n = 12)

Group	Bone Quality	Occlusal Guidance Type	Contacting Teeth
A1	D2	Canine-protected	Canine
A2	D2	Group function (2-tooth)	Canine, 1st premolar
A3	D2	Group function (3-tooth)	Canine, 1st premolar, 2nd premolar
A4	D2	Group function (posterior)	1st premolar, 2nd premolar, 1st molar
B1–B4	D3	Same as A1–A4	Same as A1–A4
C1–C4	D4	Same as A1–A4	Same as A1–A4

Notes. Bone quality categories were defined by density and Young's modulus values: D2 = dense cancellous bone (Young's modulus: 5,500 MPa); D3 = medium-density cancellous bone (Young's modulus: 1,600 MPa); D4 = low-density cancellous bone (Young's modulus: 690 MPa).

Occlusal guidance patterns were defined as follows: Canine-protected occlusion, contact limited to the canine only during lateral excursion; 2-tooth group function, contact of the canine and first premolar; 3-tooth group function, contact of the canine, first premolar, and second premolar; posterior group function, contact of the first premolar, second premolar, and first molar with no canine involvement.

Material Properties and Interface Definitions

All materials were assigned isotropic, homogeneous, and linearly elastic properties based on established literature values and experimental data [12–16]. Young's modulus values and Poisson's ratios were

selected from peer-reviewed sources to ensure computational accuracy and clinical relevance (Table 2).

Table 2
Material Properties Used in Finite Element Analysis

Material Component	Young's Modulus (MPa)	Poisson's Ratio	Reference
Cortical bone	13,700	0.30	[10]
D2 cancellous bone	5,500	0.30	[11]
D3 cancellous bone	1,600	0.30	[11]
D4 cancellous bone	690	0.30	[11]
Titanium implant	115,000	0.35	[13]
Titanium abutment	110,000	0.35	[13]
Zirconia crown	210,000	0.27	[13]

Boundary Conditions and Loading Protocols

Maxillary bone surfaces were constrained in all translational degrees of freedom (X, Y, Z directions) to simulate cranial attachment. This constraint configuration prevents rigid body motion while allowing realistic stress development within the model.

Displacement-controlled quasi-static loading conditions simulated physiological lateral jaw movements. The volunteer's mandibular movement trajectory, captured through intraoral scanning, was used as the displacement boundary condition to simulate lateral movements through contact analysis. A friction coefficient of 0.5 was applied, representing realistic contact conditions between natural enamel and zirconia surfaces.

Loading trajectories were derived from recorded mandibular movement patterns, ensuring physiologically relevant force directions and contact sequences. This approach eliminated unrealistic force magnitudes while maintaining clinically appropriate stress distributions and contact relationships.

Finite Element Analysis and Computational Processing

Tetrahedral mesh generation was performed in Abaqus 2021 software (Dassault Systèmes, France) using advanced mesh generation algorithms. Mesh density was optimized through convergence testing, with refined discretization applied to critical stress concentration areas including implant-bone interfaces, abutment connection regions, and framework support areas (Table 3).

Table 3
Finite Element Mesh Characteristics

Model Component	Node Count	Element Count	Element Type
Implants	92,821	465,739	C3D4
Abutments	21,792	102,821	C3D4
Cortical bone	182,766	936,288	C3D4
Cancellous bone	78,139	328,143	C3D4
Framework	107,869	545,748	C3D4
Crowns	125,553	626,576	C3D4

Von Mises stress distributions and framework deformation values were calculated for each experimental condition using implicit solution algorithms. Computational analysis was performed on high-performance computing systems with adequate memory allocation for large-scale finite element problems.

Data Analysis and Statistical Evaluation

Quantitative stress analysis focused on maximum von Mises stress values at critical locations including implant cervical regions, abutment-implant interfaces, and framework connection areas. Color-coded stress distribution maps facilitated visual analysis of stress concentration patterns and comparative evaluation between experimental groups.

Framework deformation was assessed through displacement magnitude calculations at predefined reference points. Statistical comparison between groups was performed using descriptive analysis and percentage change calculations to identify clinically significant differences in biomechanical behavior.

Results

Overall Stress Distribution Patterns

Stress concentration consistently localized at the implant cervical regions and abutment-implant interfaces across all experimental conditions. The Von Mises stress distribution of implants under D2 bone quality was evaluated across the four lateral guidance types (Fig. 2).

The corresponding stress distribution on the abutments highlighted that abutment components experienced the highest stress concentrations among all prosthetic elements (Fig. 3). The stress distribution on the frameworks exhibited a radial pattern originating from the abutment connection interfaces (Fig. 4).

Bone Quality Effects and Lateral Guidance Pattern Influence

Compared with canine-protected occlusion (113.65 MPa), the maximum implant stress at position 15 under three-tooth group function (165.47 MPa) increased by 45.6%; at position 25, the increase was 75.6% (from 115.14 MPa to 202.23 MPa). Under D4 bone quality, the mean framework deformation for posterior group function reached 0.0496 mm—an increase of 49% compared with 0.0333 mm under D2 canine-protected conditions (Fig. 5).

Table 4
Maximum Von Mises Stress Values (MPa) by Bone Quality Under Canine-Protected Occlusion

Implant Position	D2 Bone Quality	D3 Bone Quality	D4 Bone Quality	Percentage Reduction (D2→D4)
Position 15	113.65	104.50	96.35	15.2%
Position 12	150.24	144.64	126.77	15.6%
Position 22	149.00	110.34	108.01	27.5%
Position 25	115.14	105.00	90.78	21.2%

Lateral Guidance Pattern Influence

Canine-protected occlusion consistently demonstrated superior biomechanical performance compared to group-function alternatives across all bone quality conditions (Fig. 6). This finding supports clinical preferences for canine guidance in natural dentition and extends these principles to implant-supported prostheses.

Position 12 exhibited the most extensive stress distribution during canine-guided lateral movements, with stress concentration areas significantly larger than other implant positions. This pattern reflects the biomechanical role of canine teeth in lateral force management and suggests that position 12 experiences the highest mechanical demands during lateral jaw movements.

Table 5
Maximum Von Mises Stress Values (MPa) Under D2 Bone Quality Across Lateral Guidance Patterns

Component	Canine Protection	2-Tooth Group	3-Tooth Group	Posterior Group
Position 15 Implant	113.65	125.80	165.47	156.03
Position 12 Implant	150.24	163.21	198.70	158.44
Position 15 Abutment	132.20	141.74	191.03	201.21
Position 12 Abutment	230.09	243.34	259.88	210.07

The maximum stress concentration occurred at position 12 abutment during three-tooth group function (259.88 MPa), representing approximately 63% of titanium alloy yield strength (410 MPa). While this value remains below immediate failure thresholds, repeated cyclic loading at these stress levels may contribute to fatigue failure mechanisms observed clinically.

Framework Deformation Analysis

Framework deformation patterns demonstrated inverse relationships with bone quality, confirming biomechanical principles relating material stiffness to structural deflection under load. Higher bone density (D2) provided greater support rigidity, resulting in minimal framework deformation but increased stress concentration at implant-abutment interfaces.

Table 6
Framework Deformation Values (mm) Across Experimental Conditions

Bone Quality	Canine Protection	2-Tooth Group	3-Tooth Group	Posterior Group
D2	0.0333	0.0355	0.0405	0.0451
D3	0.0365	0.0374	0.0430	0.0476
D4	0.0378	0.0384	0.0449	0.0496

Progressive increases in framework deformation correlated positively with both reduced bone quality and increased numbers of cuspal contacts in group-function patterns. Maximum deformation occurred under D4 bone conditions with posterior group function (0.0496mm), representing a 49% increase compared to optimal conditions (D2 bone with canine protection).

Position-Specific Stress Analysis

Individual implant positions demonstrated distinct stress patterns reflecting their roles in overall prosthetic function. Anterior positions (12, 22) experienced higher stress magnitudes during lateral movements compared to posterior positions (15, 25), consistent with their primary load-bearing responsibilities during lateral guidance.

Position 22 showed unique behavior patterns, with stress values remaining relatively stable across different guidance patterns during right lateral movements. This finding suggests that contralateral positioning during working-side lateral movements results in reduced loading compared to working-side positions.

Posterior positions (15, 25) demonstrated progressive stress increases as guidance patterns shifted from canine protection toward posterior group function. This transition effectively transferred loading responsibilities from anterior canine positions to posterior implant sites, potentially exceeding optimal loading thresholds for angled implant configurations.

Discussion

Occlusal design plays a critical role in the long-term stability of implant-supported rehabilitations in edentulous patients, with lateral occlusion being particularly influential. However, lateral guidance design in edentulous implant prostheses remains controversial, with no consensus-based clinical guidelines currently available. Commonly advocated concepts include balanced occlusion, group function, and canine-protected occlusion, and their indications continue to be debated. Penarrocha-Diago et al. suggested that occlusal schemes should be adapted according to opposing dentition, recommending bilateral balanced occlusion against complete dentures and either group function or canine guidance against natural dentition [17]. In contrast, clinical studies by Abduo et al. [18] and Miralles et al. [19] reported no significant differences between group function and canine guidance in terms of patient comfort or long-term outcomes, indicating that both schemes may be clinically acceptable.

For All-on-4 restorations specifically, previous finite element studies have produced conflicting results. Turker et al. [20] reported lower stress in abutments, screws, and superstructures under group function, whereas a separate analysis demonstrated reduced stress in implants and peri-implant bone under canine-protected occlusion. Although similar computational methods were applied, these studies focused on different structural components, suggesting that occlusal scheme–related stress responses vary among bone tissue, implants, abutments, screws, and prosthetic frameworks. This heterogeneity highlights the complexity of biomechanical behavior in All-on-4 systems and underscores the need for comprehensive analyses that simultaneously consider multiple components during functional movements.

Using three-dimensional finite element analysis under dynamic mandibular displacement, the present study evaluated stress distribution in implants, abutments, frameworks, and surrounding bone under different lateral guidance designs and bone quality conditions. The results demonstrated that canine-protected occlusion was associated with more favorable stress distribution at the implant–abutment interface and within the prosthetic framework during lateral excursions, whereas group function designs involving posterior contacts generated higher stress concentrations, particularly under three-tooth guidance. Stress at the 15 and 25 implant sites increased by up to 166% under group function, suggesting a potentially elevated risk of mechanical complications. Abutments consistently exhibited the highest stress concentration among all components, consistent with clinical reports identifying abutment-related failures as common technical complications in All-on-4 restorations [21]

Stress magnitude was further influenced by implant position, angulation, and bone quality. Decreasing bone density was associated with reduced stress concentration at the implant–abutment interface. This phenomenon is not a biomechanical advantage; it is primarily attributed to increased micro-motion and stress shielding caused by poor bone quality, which is accompanied by increased framework deformation and structural compliance [22]. Excessive deformation may compromise prosthetic stability and increase fatigue risk over time. Collectively, these findings suggest that lateral occlusal design represents a critical and potentially modifiable factor in the biomechanical performance of All-on-4 prostheses. In the absence of clinical consensus regarding lateral guidance, canine-protected occlusion appears to offer biomechanical advantages during lateral movements. Nevertheless, this study has

several limitations. The finite element model was based on a single healthy volunteer, which fails to reflect the complex mechanical environments of actual edentulous patients typically presenting with alveolar bone resorption and soft tissue variations; therefore, it provides relative trends rather than absolute clinical values [23, 24]. Regarding the simplified bone simulation, the study adjusted the cancellous bone elastic modulus but maintained a constant cortical bone thickness, which may overestimate implant stability in low-density bone (D4) where cortical thinning is common. Furthermore, all materials were assumed to be isotropic and linear elastic, and the implant-bone interface was defined as perfectly bonded. This idealized osseointegration ignores potential micro-motion during immediate loading, potentially leading to an underestimation of stress. Additionally, while displacement-controlled quasi-static loading eliminates artificial force assumptions, the dynamic resultant reaction forces generated during displacement were not reported. Finally, the simulation did not account for parafunctional movements, such as bruxism or clenching, which could generate significantly higher stresses. Future studies incorporating patient-specific anatomy, diverse loading conditions, and time-dependent adaptive responses are required to support the development of evidence-based occlusal guidelines for edentulous All-on-4 implant rehabilitations.

Conclusion

Using three-dimensional finite element analysis under displacement-controlled quasi-static loading, this study showed that lateral guidance design significantly affects stress distribution in maxillary edentulous All-on-4 restorations. Canine-protected occlusion reduced stress concentration in implants and multi-unit abutments compared with group function, whereas increasing the number of guiding cusps in group function progressively increased stress. The highest stress during lateral guidance consistently occurred at the multi-unit abutment. In addition, reduced alveolar bone density increased framework deformation, suggesting a higher risk of mechanical complications. These findings provide biomechanical evidence to inform occlusal design in All-on-4 rehabilitations, where clinical consensus remains limited.

Declarations

Ethics approval and consent to participate

This study conforms to the Declaration of Helsinki and was approved by the Medical Ethics Committee of the Affiliated Stomatological Hospital of Guizhou Medical University (Ethics Approval No.2025-15).A single healthy volunteer provided informed consent for digital imaging and mandibular movement recording procedures.

Consent for publication

Not applicable.

Competing Interests

The authors have no conflicts of interest relevant to this article.

Funding

This work was supported by National Natural Science Foundation of

Author Contribution

Y-R.S.: Study design, data collection and analysis, manuscript writing;H-J.L.: Data collection, statistical analysis, manuscript revision;S-Y.L., X.Z., Q.D.: Study supervision, manuscript review and final approval.All authors read and approved the final manuscript.

Acknowledgements

Not applicable.

Data Availability

The datasets used and analysed during the current study are available from the corresponding author on reasonable request.

References

1. Kilic K, Sayin B, Özer F, Akin S. Influence of Conventional Complete Dentures and Different Attachment Types in Implant-Supported Overdentures on Quality of Life and Nutritional Status in Edentulous Geriatric Patients. Int J Prosthodont. 2021;34:7–12.
2. Kutkut A, Bertoli E, Frazer R, Pinto-Sinai G, Fuentealba Hidalgo R, Studts J. A systematic review of studies comparing conventional complete denture and implant retained overdenture. J prosthodontic Res. 2018;62(1):1–9.
3. Bornstein MM, Ho JKC, Yeung AWK, Tanaka R, Li JQ, Jacobs R. A Retrospective Evaluation of Factors Influencing the Volume of Healthy Maxillary Sinuses Based on CBCT Imaging. Int J Periodontics Restor Dent. 2019;39(2):187–93.
4. Zhang Y, Tang X, Zhang Y, Cao C. A network meta-analysis comparing treatment modalities of short and long implants in the posterior maxilla with insufficient bone height. BMC Oral Health. 2024;24(1):1574.

5. Maló P, Rangert B, Nobre M. All-on-Four immediate-function concept with Brånemark System implants for completely edentulous mandibles: a retrospective clinical study. Clin Implant Dent Relat Res. 2003;5(Suppl 1):2–9.
6. Maló P, de Araújo Nobre M, Lopes A, Ferro A, Nunes M. The All-on-4 concept for full-arch rehabilitation of the edentulous maxillae: A longitudinal study with 5–13 years of follow-up. Clin Implant Dent Relat Res. 2019;21(4):538–49.
7. Gross M, Gracis S, Gamborena I. The science and art of occlusion and oral rehabilitation. Quintessence publishing; 2015. pp. 303–42.
8. Bashutski JD, D'Silva NJ, Wang HL. Implant compression necrosis: current understanding and case report. J Periodontol. 2009;80(4):700–4.
9. Ferreira PW, Nogueira PJ, Nobre MAA, Guedes CM, Salvado F. Impact of Mechanical Complications on Success of Dental Implant Treatments: A Case-Control Study. Eur J dentistry. 2022;16(1):179–87.
10. Kapoor S, Rodrigues S, Mahesh M, Shetty T, Pai U, Saldanha S et al. Evaluation of Stress Generated with Different Abutment Materials and Angulations under Axial and Oblique Loading in the Anterior Maxilla: Three-Dimensional Finite Element Analysis. International journal of dentistry 2021; 2021:9205930.
11. Misch CE. Contemporary Implant Dentistry. 3rd ed. Mosby Elsevier; 2008. pp. 130–46.
12. Isidor F. Influence of forces on peri-implant bone. Clin Oral Implants Res. 2006;17(Suppl 2):8–18.
13. Mourya A, Nahar R, Mishra SK, Chowdhary R. Stress distribution around different abutments on titanium and CFR-PEEK implant with different prosthetic crowns under parafunctional loading: A 3D FEA study. J oral biology Craniofac Res. 2021;11(2):313–20.
14. Comuzzi L, Ceddia M, Di Pietro N, Inchingolo F, Inchingolo AM, Romasco T et al. Crestal and Subcrestal Placement of Morse Cone Implant-Abutment Connection Implants: An In Vitro Finite Element Analysis (FEA) Study. Biomedicines 2023; 11(11).
15. Brandão de Holanda KA, Armini Caldas R, Amaral M, da Silva Concilio LR, Pino Vitti R. Biomechanical evaluation of anterior implants associated with titanium and zirconia abutments and monotype zirconia implants. J prosthodontic Res. 2021;65(1):73–7.
16. Brune A, Stiesch M, Eisenburger M, Greuling A. The effect of different occlusal contact situations on peri-implant bone stress - A contact finite element analysis of indirect axial loading. Materials science & engineering C, Materials for biological applications. 2019; 99:367 – 73.
17. Penarrocha-Diago M, Penarrocha-Diago M, Zaragozí-Alonso R, Soto-Penaloza D, On Behalf Of The Ticare Consensus M. Consensus statements and clinical recommendations on treatment indications, surgical procedures, prosthetic protocols and complications following All-On-4 standard treatment. 9th Mozo-Grau Ticare Conference in Quintanilla, Spain. Journal of clinical and experimental dentistry,. 2017; 9(5):e712-e5.
18. Abduo J, Tennant M, McGeachie J. Lateral occlusion schemes in natural and minimally restored permanent dentition: a systematic review. J Rehabil. 2013;40(10):788–802.

19. Gutiérrez MF, Miralles R, Fuentes A, Cavada G, Valenzuela S, Santander H, et al. The effect of tooth clenching and grinding on anterior temporalis electromyographic activity in healthy subjects. Cranio J Craniomandib Pract. 2010;28(1):43–9.
20. Türker N, Büyükkaplan US, Sadowsky SJ, Özarslan MM. Finite Element Stress Analysis of Applied Forces to Implants and Supporting Tissues Using the All-on-Four Concept with Different Occlusal Schemes. J prosthodontics: official J Am Coll Prosthodontists. 2019;28(2):185–94.
21. Tuminelli FJ, Jivraj S, Bongard S, Powell D. Prosthetic Complications with Immediately Loaded, Full-Arch, Fixed Implant-Supported Prostheses. In: *Graftless Solutions for the Edentulous Patient.* edn. Edited by Jivraj S. Cham: Springer International Publishing; 2023: 447 – 72.
22. Mizusawa K, Shin C, Okada D, Ogura R, Komada W, Saleh O, et al. The investigation of the stress distribution in abutment teeth for connected crowns. J Dent Sci. 2021;16(3):929–36.
23. Wang Q, Zhao Z, Li J, Zhao R, Zhou M, Tang K, et al. In vivo evaluation of T-Scan in quantifying occlusal contact. J Rehabil. 2024;51(9):1675–83.
24. Iyota K, Mizutani S, Oku S, Asao M, Futatsuki T, Inoue R et al. A Cross-Sectional Study of Age-Related Changes in Oral Function in Healthy Japanese Individuals. Int J Environ Res Public Health 2020; 17(4).

Figures

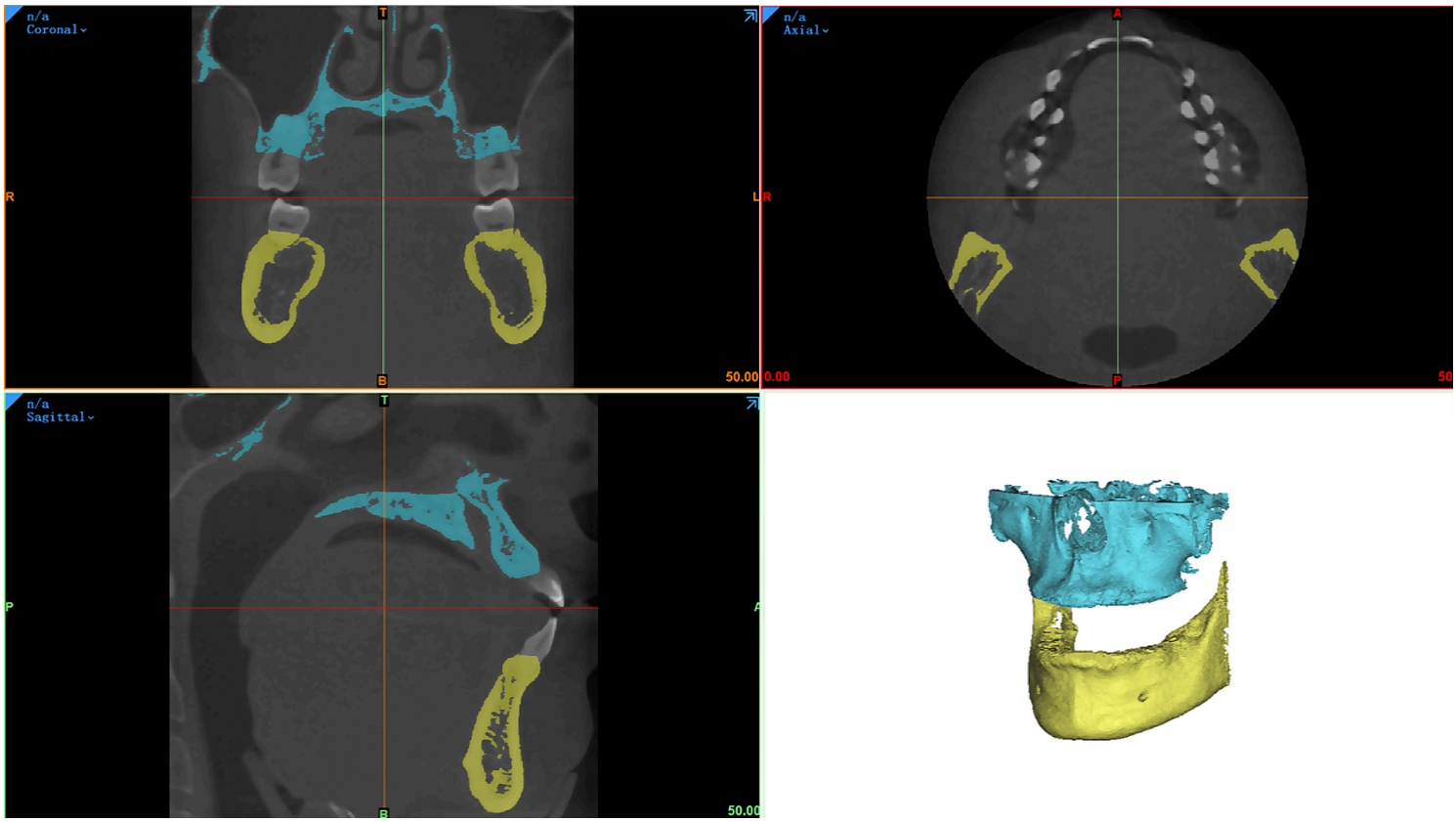


Figure 1

Mimics Extraction of Maxillary and Mandibular Jawbones

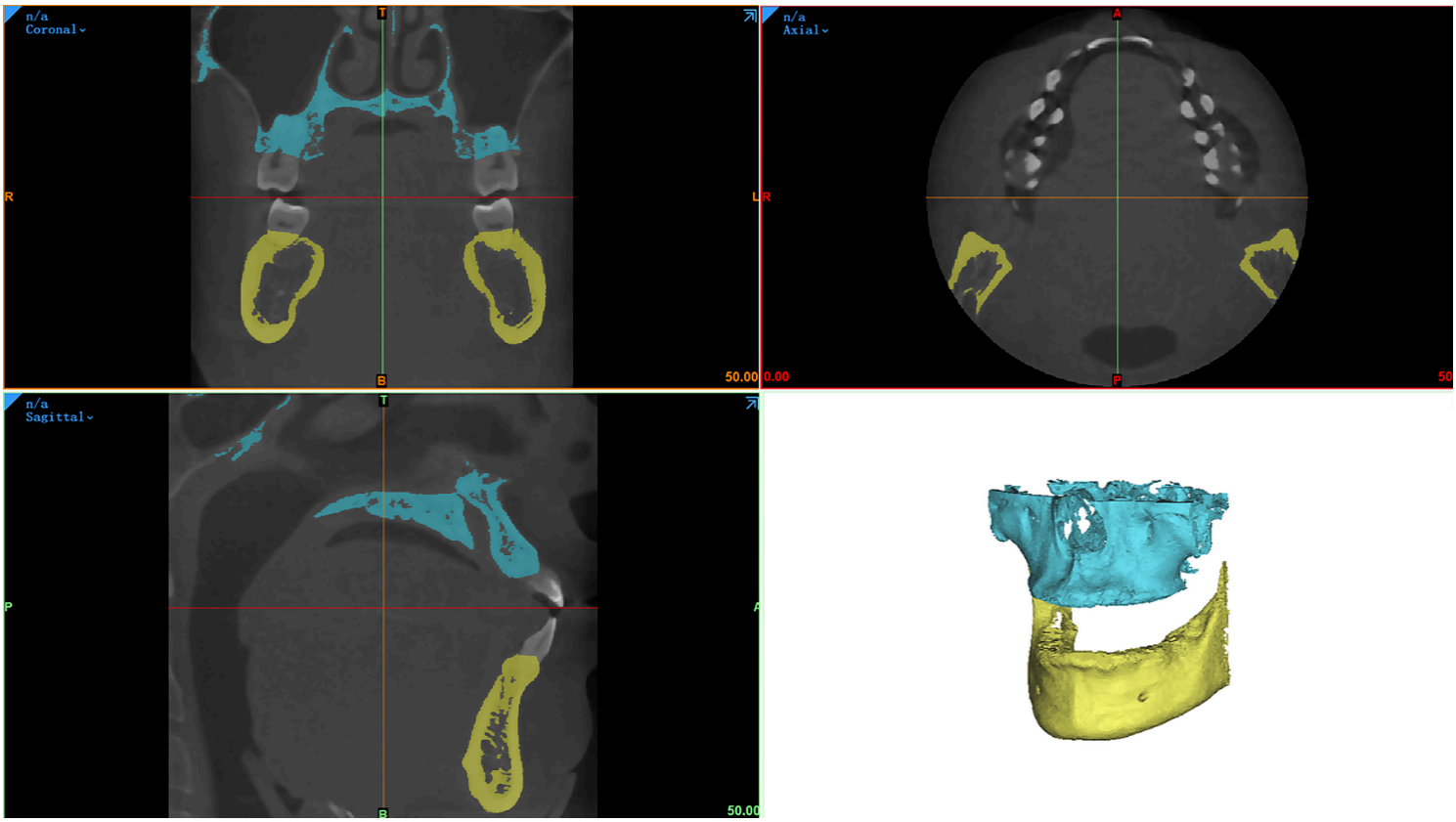


Figure 1

Mimics Extraction of Maxillary and Mandibular Jawbones

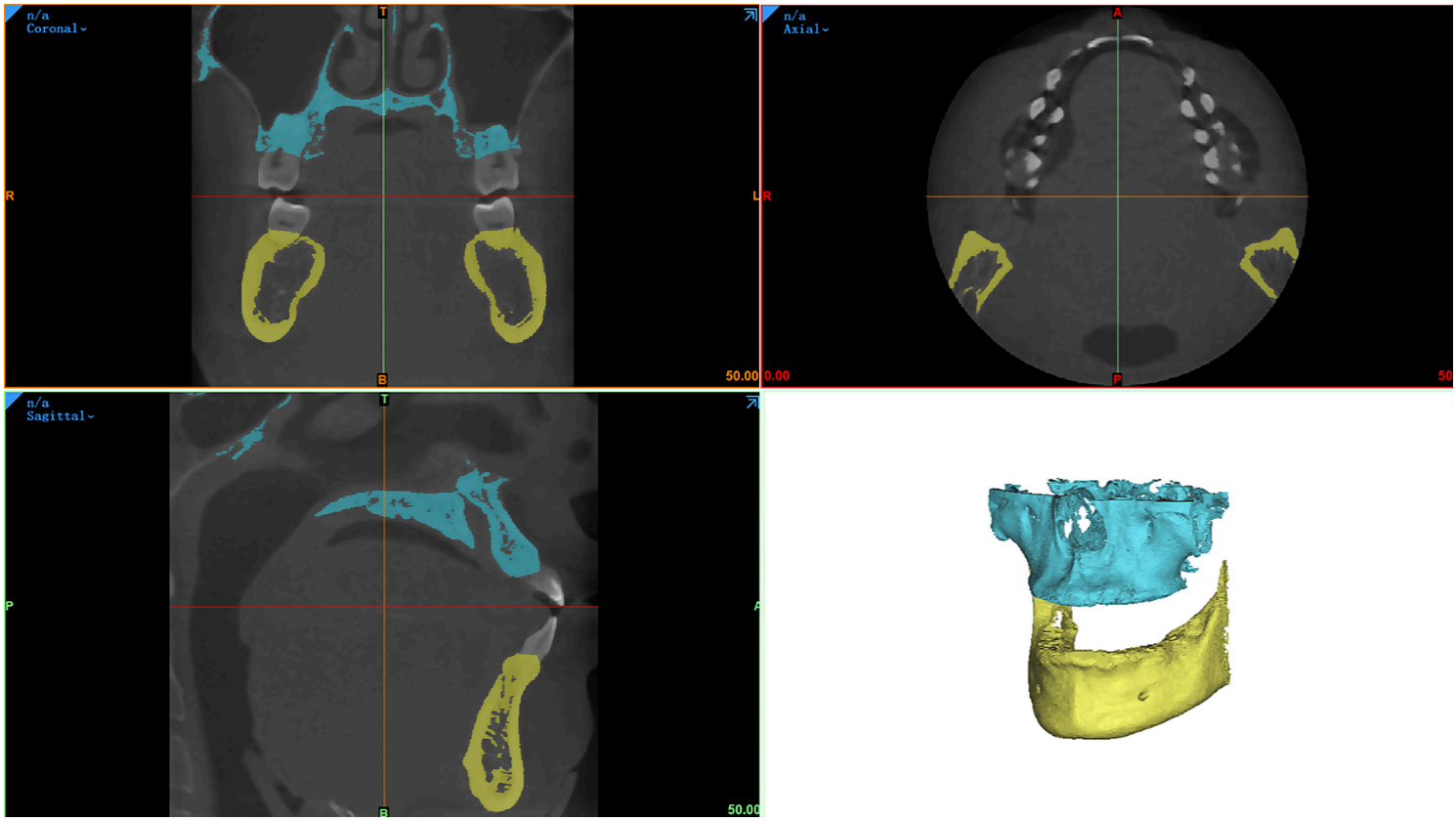
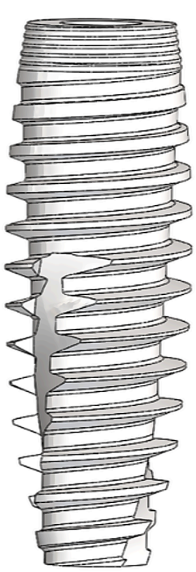


Figure 1

Mimics Extraction of Maxillary and Mandibular Jawbones



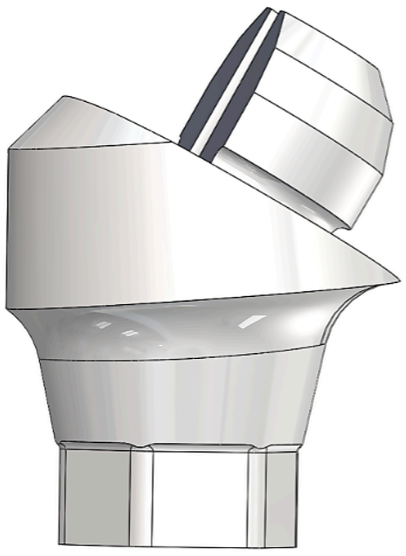


Figure 2

NobelActive Implant and 30° Angled Abutment

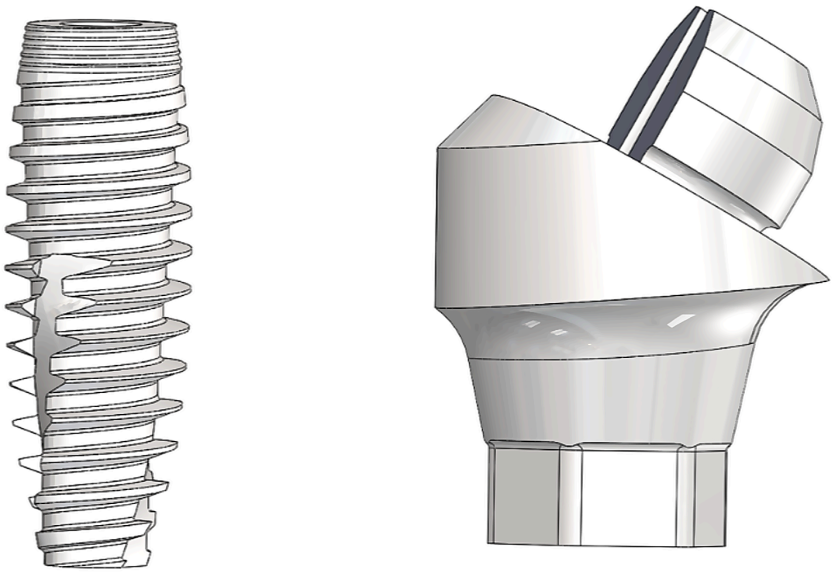


Figure 2

NobelActive Implant and 30° Angled Abutment

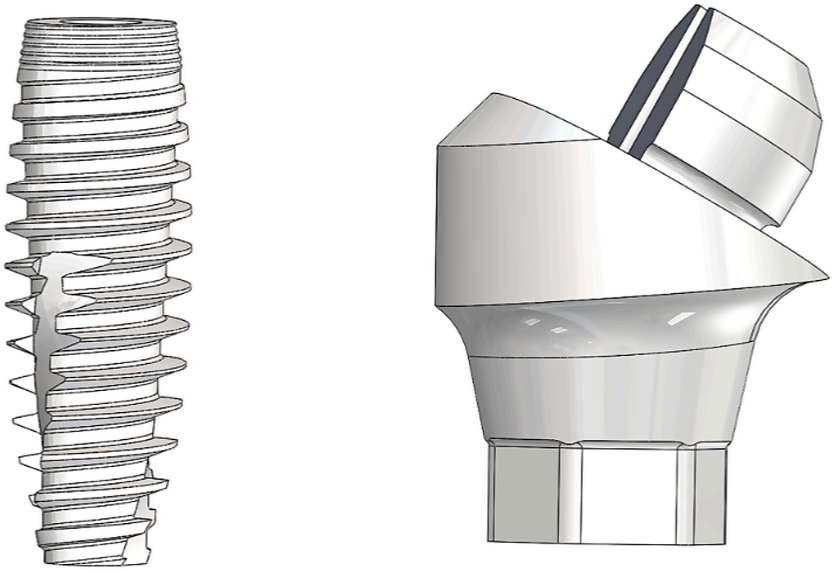


Figure 2

NobelActive Implant and 30° Angled Abutment

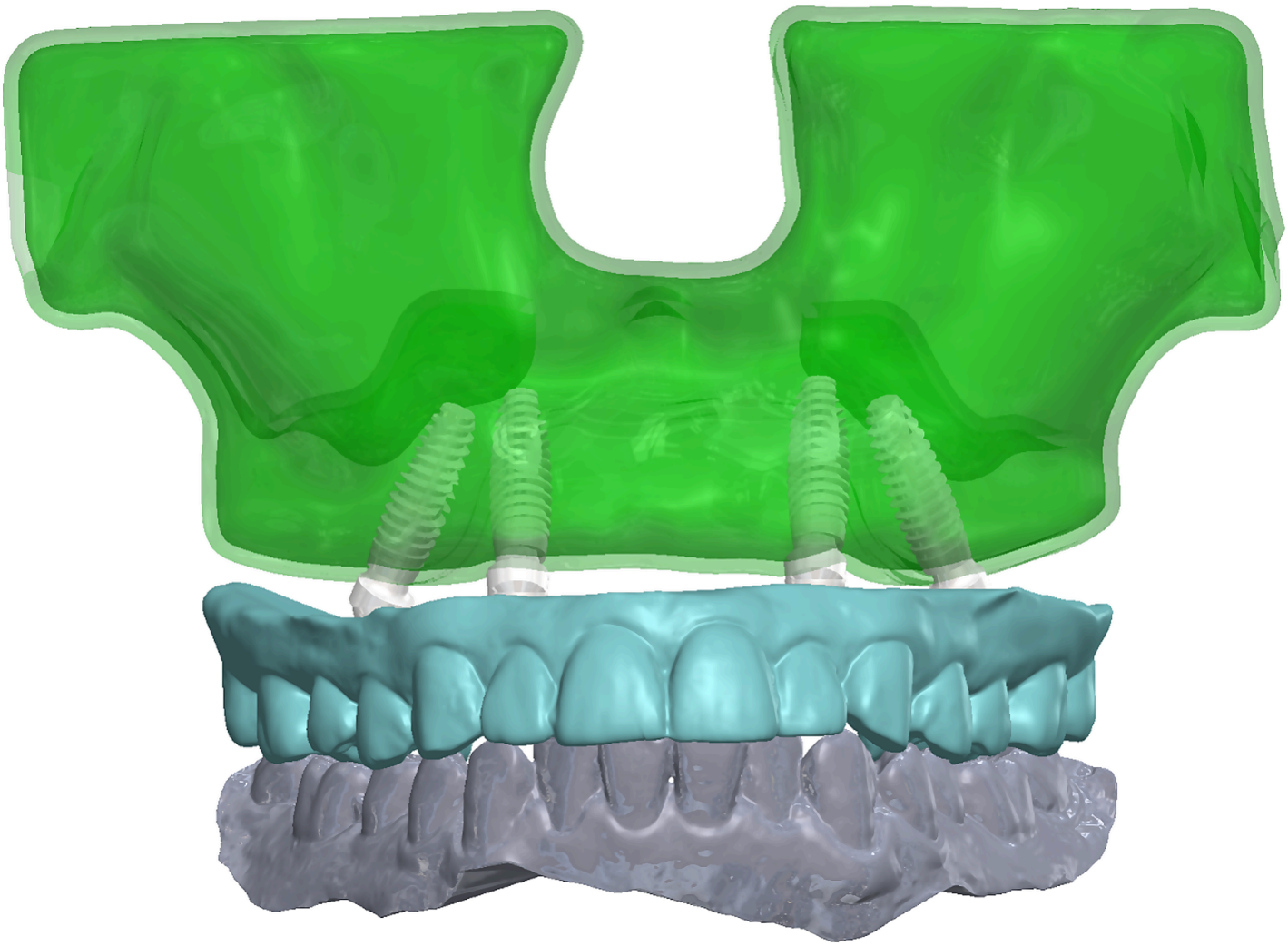


Figure 3

Fully Assembled Solid Model in SolidWorks Software

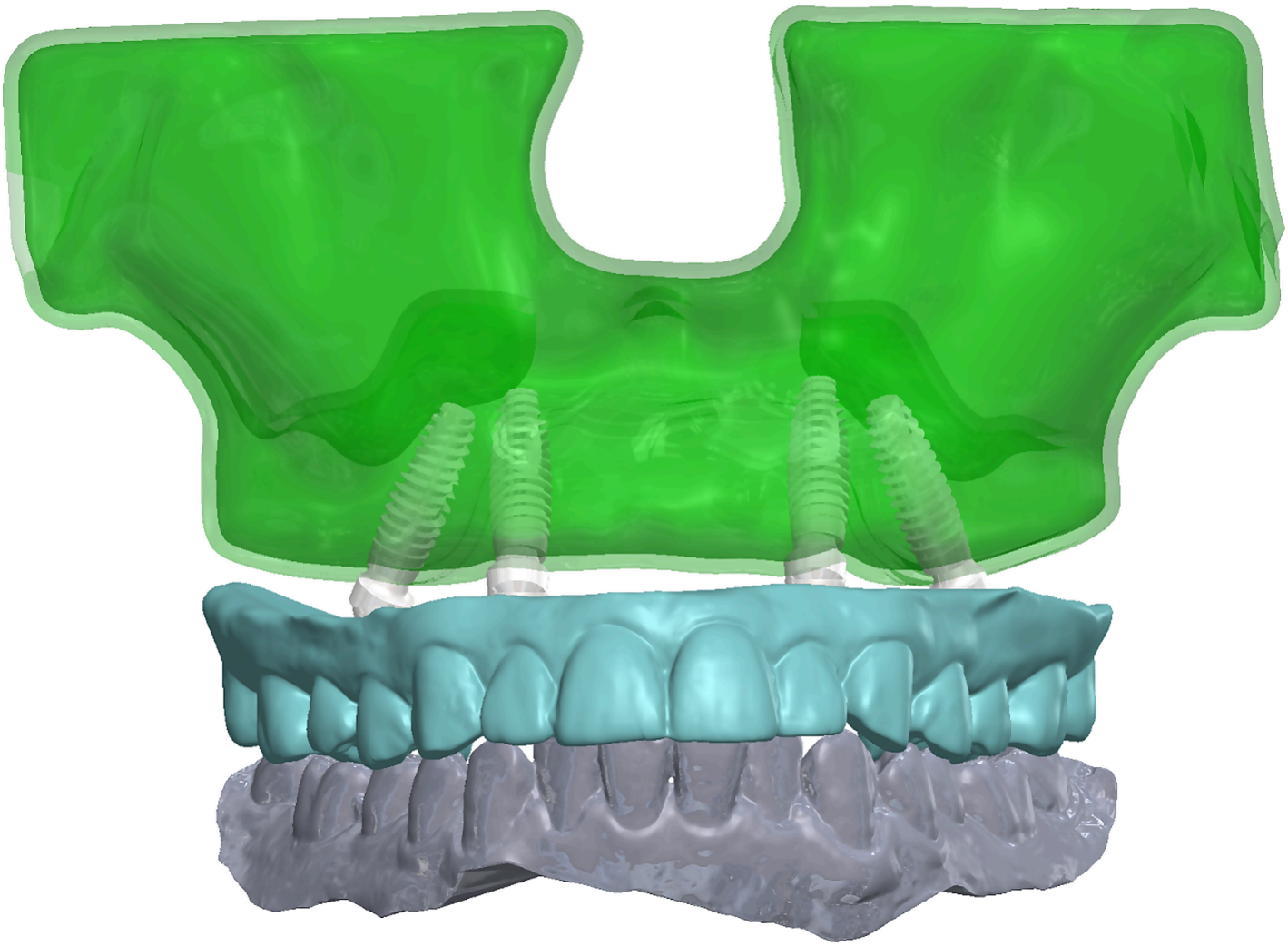


Figure 3

Fully Assembled Solid Model in SolidWorks Software

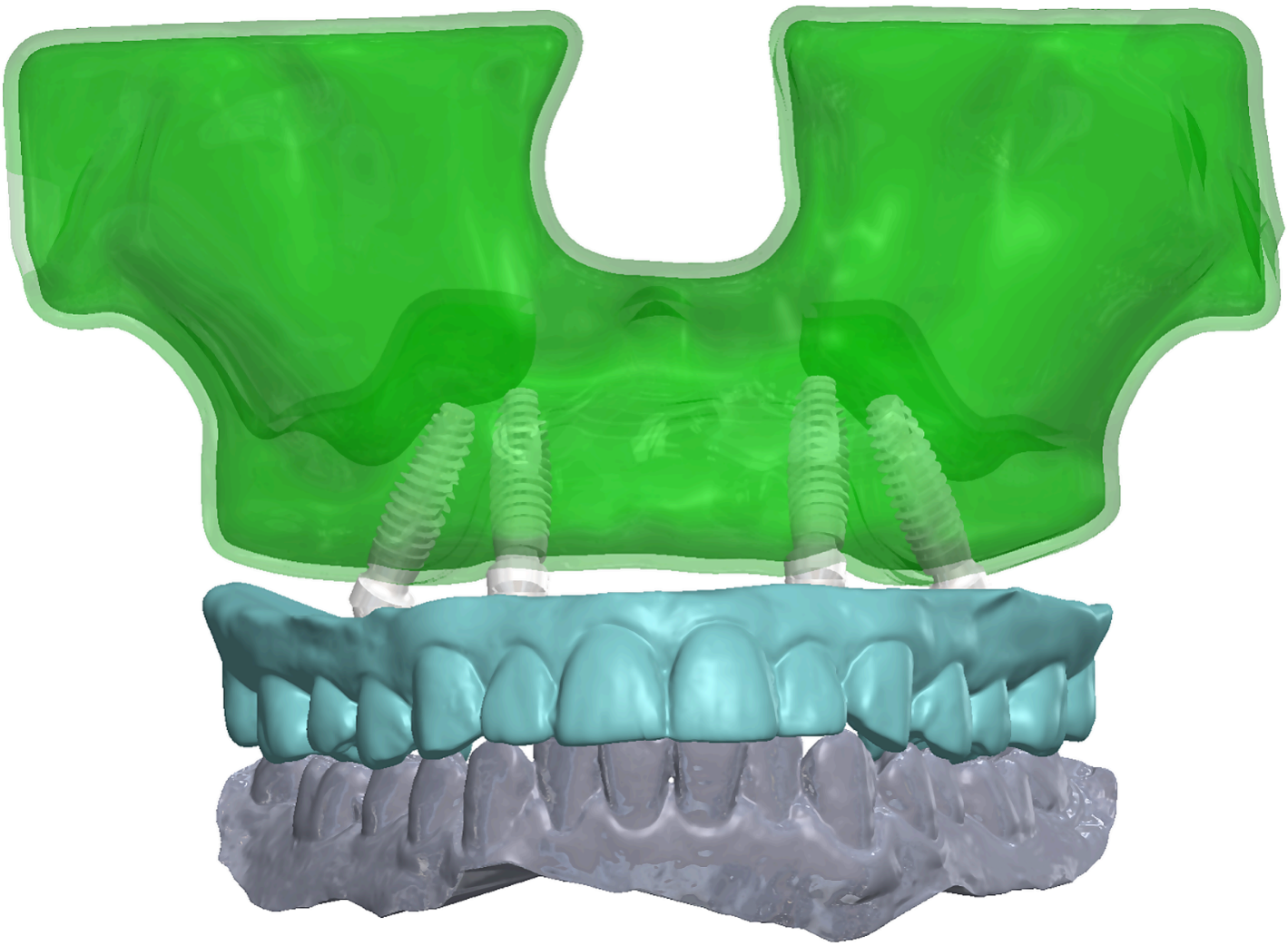


Figure 3

Fully Assembled Solid Model in SolidWorks Software

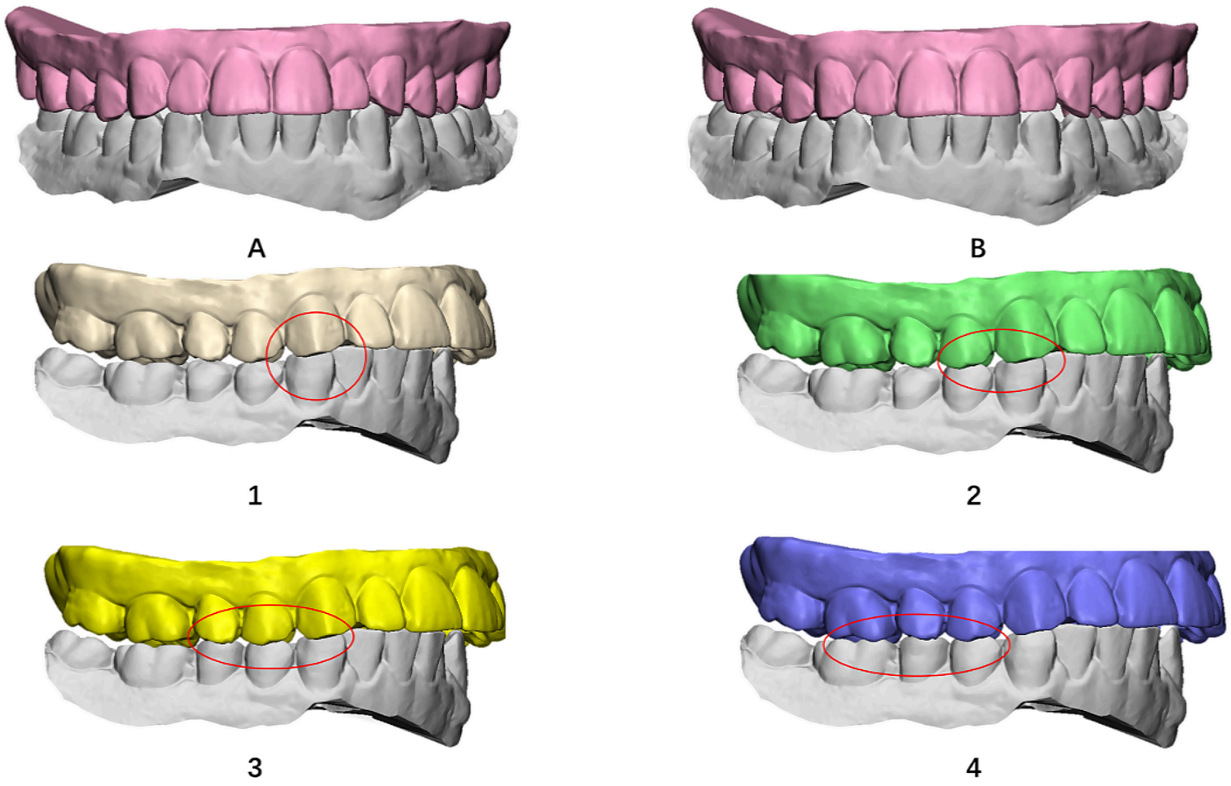


Figure 4

Volunteer's Centric Occlusion, Lateral Occlusal Movements, and Four Different Conditions

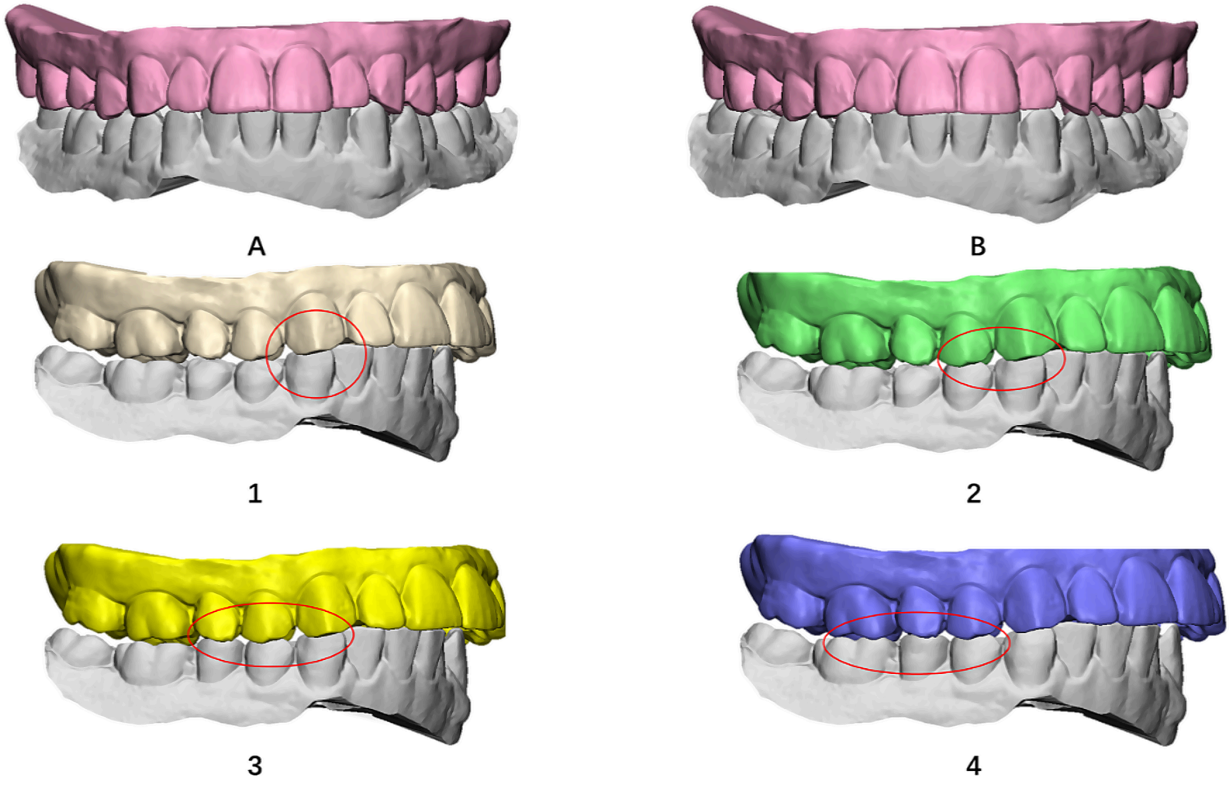


Figure 4

Volunteer's Centric Occlusion, Lateral Occlusal Movements, and Four Different Conditions

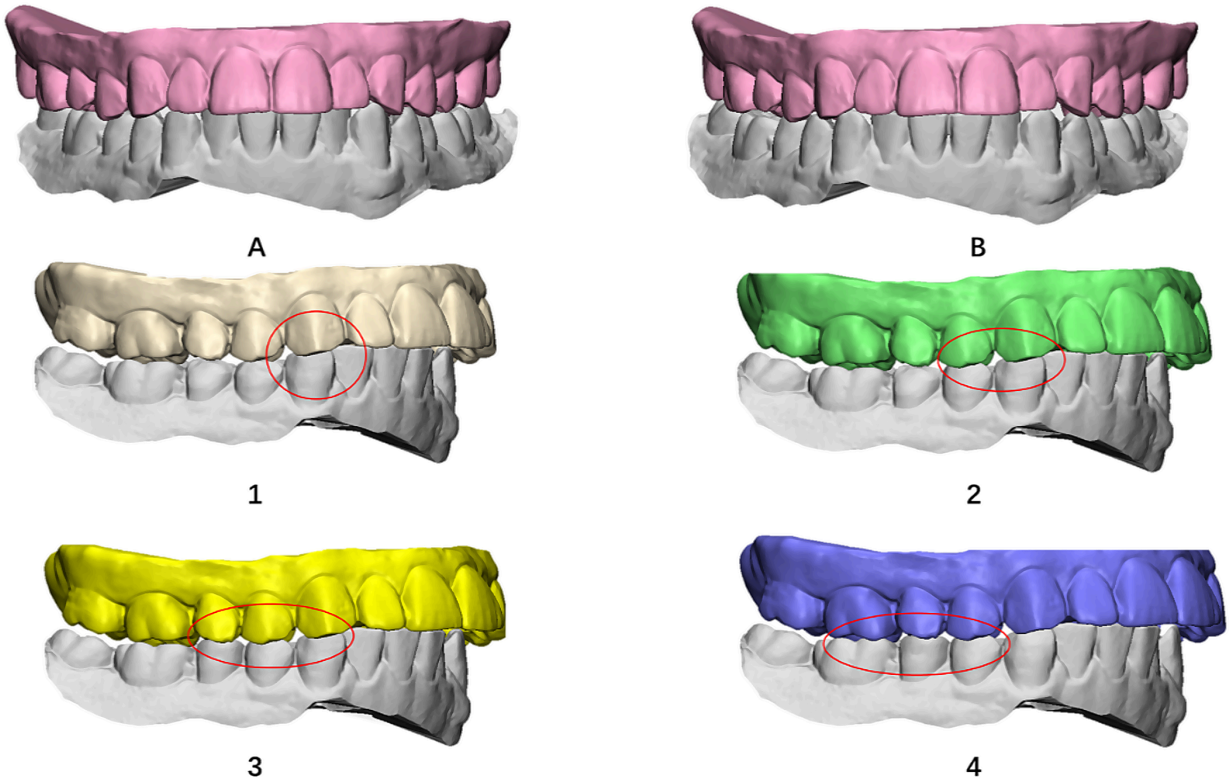


Figure 4

Volunteer's Centric Occlusion, Lateral Occlusal Movements, and Four Different Conditions

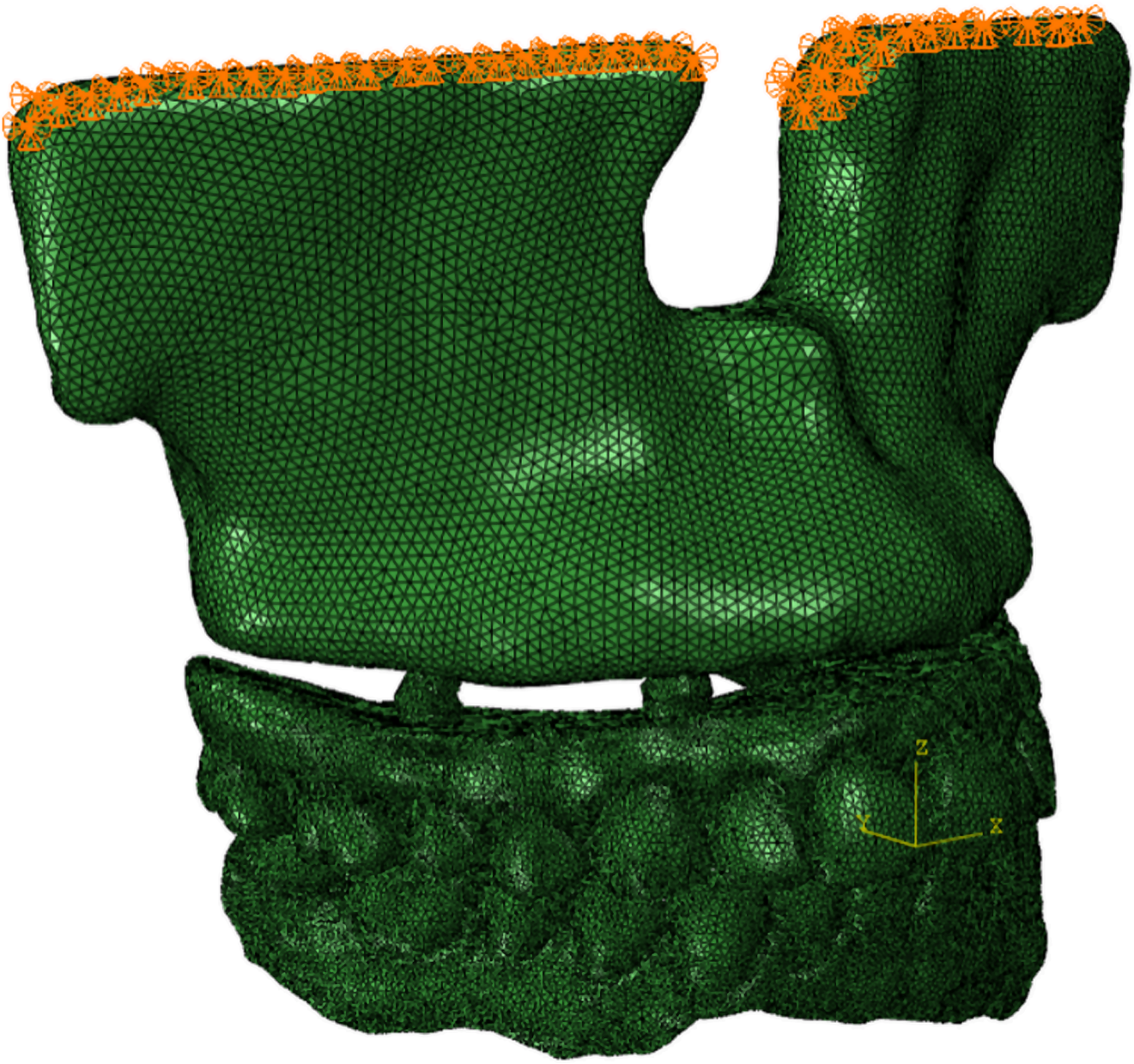


Figure 5

Maxillary Constraint Image

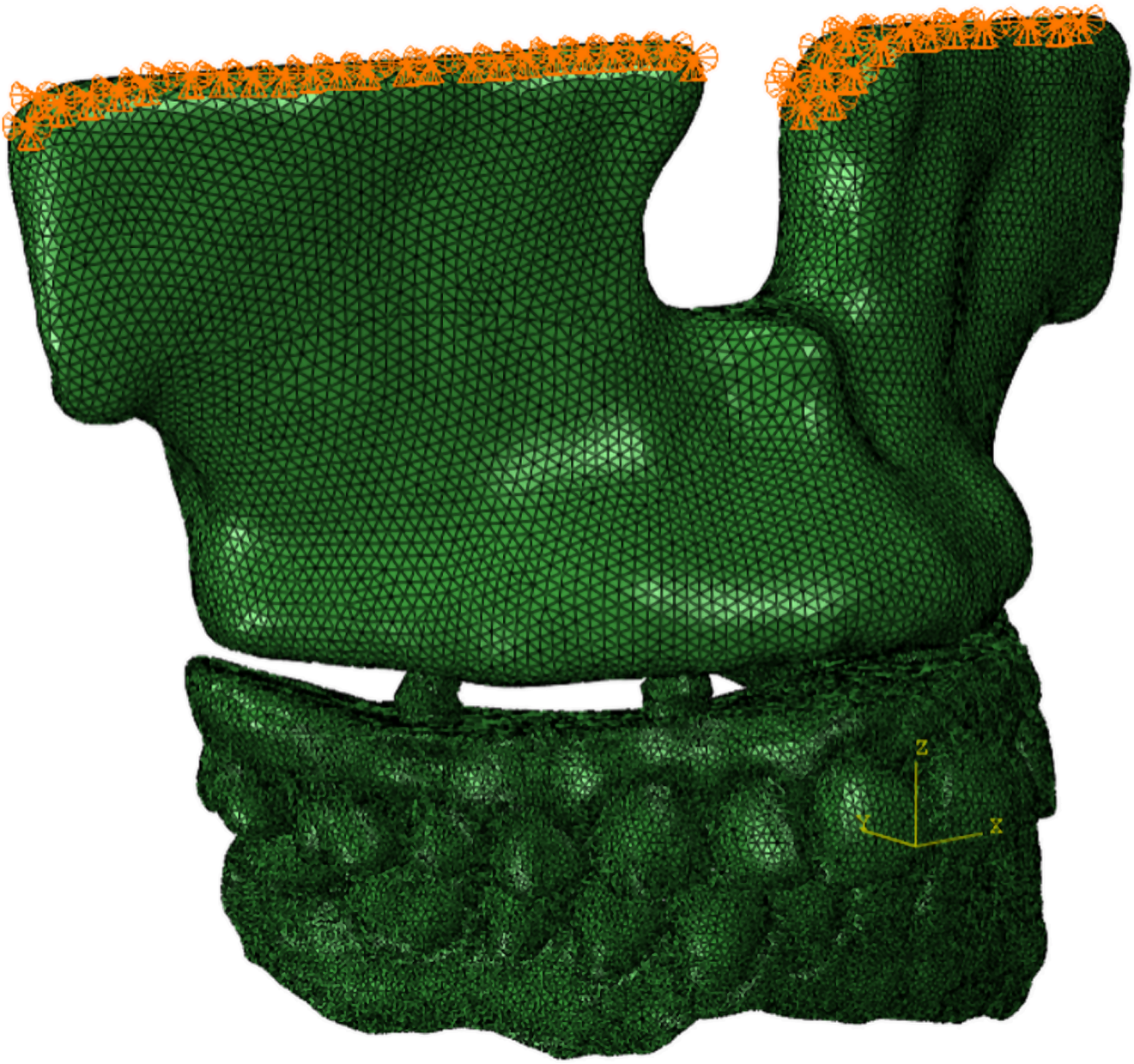


Figure 5

Maxillary Constraint Image

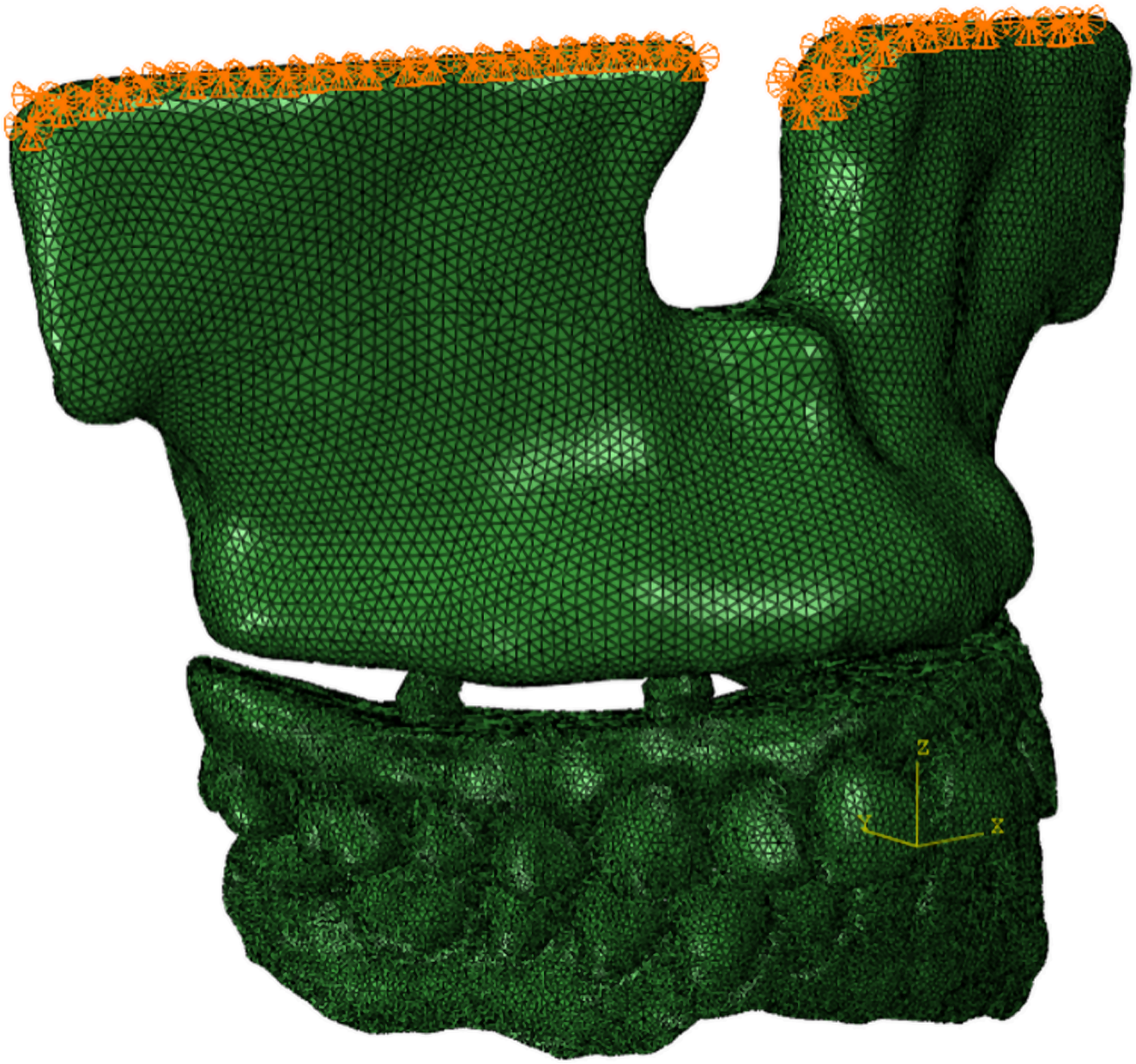


Figure 5

Maxillary Constraint Image

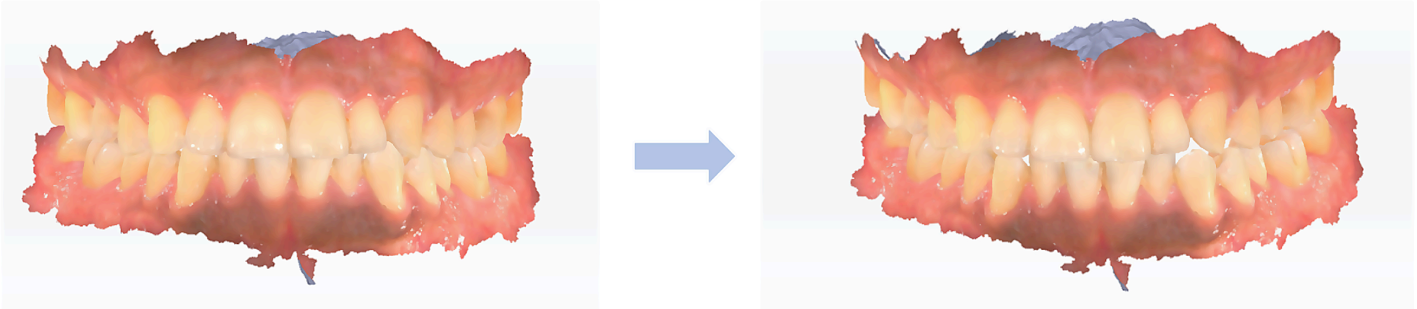


Figure 6

Volunteer’s Lateral Occlusal Movement Trajectory

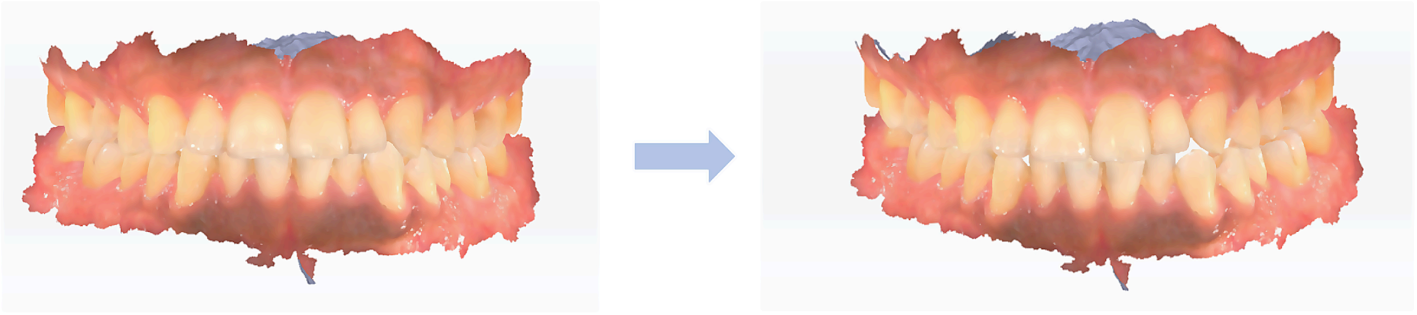


Figure 6

Volunteer’s Lateral Occlusal Movement Trajectory

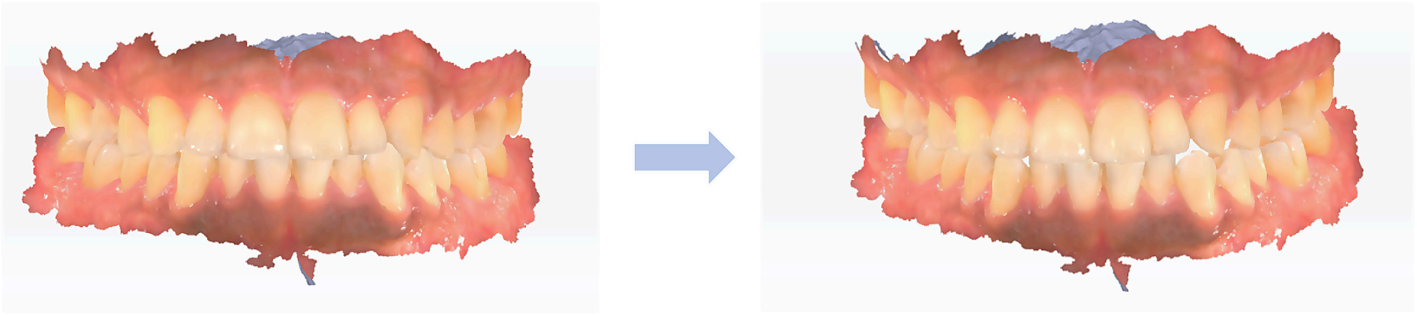


Figure 6

Volunteer’s Lateral Occlusal Movement Trajectory